Accurate measurement of elemental impurities in metals and metal alloys using triple quadrupole ICP-MS

Authors: Marcus Manecki, Daniel Kutscher and Shona McSheehy Ducos;
Thermo Fisher Scientific, Bremen, Germany

Introduction

Material properties are critical to their successful use in modern applications. Specific mechanical or chemical properties are often dependent on the presence and level of certain elements in the material. As a large proportion of construction materials are based on metallurgical products, it is critical to understand the concentrations of the trace elements in these pure metals or alloys. For example, nickel alloys are used in the aerospace industry due to their unique properties such as withstanding high temperatures and exhibiting low creep. These properties make the material ideal for the construction of turbine blades. However, it is crucial to control impurities (for example selenium), as these impurities may cause weaknesses in the blades that can lead to fracturing and, ultimately, total failure.

Another important metal is zirconium, which is often used if resistivity against high temperatures or highly corrosive environments is required. Zirconium is particularly favored for the construction of nuclear fuel rod casing, due to its low cross section for neutron capture. Nuclear grade zirconium may be blended with low amounts of e.g. tin, niobium, chromium or nickel in order to improve its mechanical properties and corrosion resistance. The presence of cadmium, even at trace levels, has to be avoided, since cadmium is known for its neutron absorbing properties and would hence negate the intended properties of the casing for this application.

ThermoFisher
SCIENTIFIC

As highlighted by the aforementioned examples, impurities found in the metals need to be tightly controlled in order to establish and maintain particular material characteristics. While some techniques, such as Laser Ablation (LA) ICP-MS or Glow Discharge Mass Spectrometry (GD-MS), use direct sampling of solid material, dissolving the metal or alloy is also a feasible way for the analysis of impurities. However, due to the large contribution of the metal to the sample matrix (often up to 1,000 ppm), the analysis of impurities found at trace levels is challenging due to the formation of spectral interferences.

Single quadrupole (SQ) ICP-MS is, in many cases, not able to fully resolve the above mentioned interferences, even if reactive gases and subsequent reactions in a collision/reaction cell (CRC) system are applied. Even for high resolution (HR) ICP-MS, the removal of polyatomic interferences such as oxides from zirconium or molybdenum is highly challenging as the required resolution is often well above 10,000. The use of a triple quadrupole (TQ) ICP-MS, such as the Thermo Scientific™ iCAP™ TQ ICP-MS, can overcome these interferences, since a mass filtering step ahead of the CRC enables more selective and efficient interference removal.

One of the most effective measurement modes of TQ-ICP-MS is referred to 'TQ mass shift mode' where the analyte is subjected to a chemical reaction and is analyzed after a shift to a different (interference free) mass. The general working principle of a TQ-ICP-MS system in TQ mass shift mode is:

Q1 rejects unwanted ions and preselects the analyte. This first stage of mass filtration rejects precursors and ions with the same *m/z* ratio as the product ion.

Optimal reaction conditions in Q2 are achieved through the selection of the appropriate measurement mode, which for the iCAP TQ ICP-MS is simplified using the Reaction Finder feature of the Thermo Scientific Qtegra™ Intelligent Scientific Data Solution™ (ISDS) Software.

Q3 isolates the product ion of the analyte and removes any remaining interferences through a second stage of mass filtration.

The principle of TQ mass shift mode is demonstrated for the ^{80}Se isotope in a nickel matrix in Figure 1.
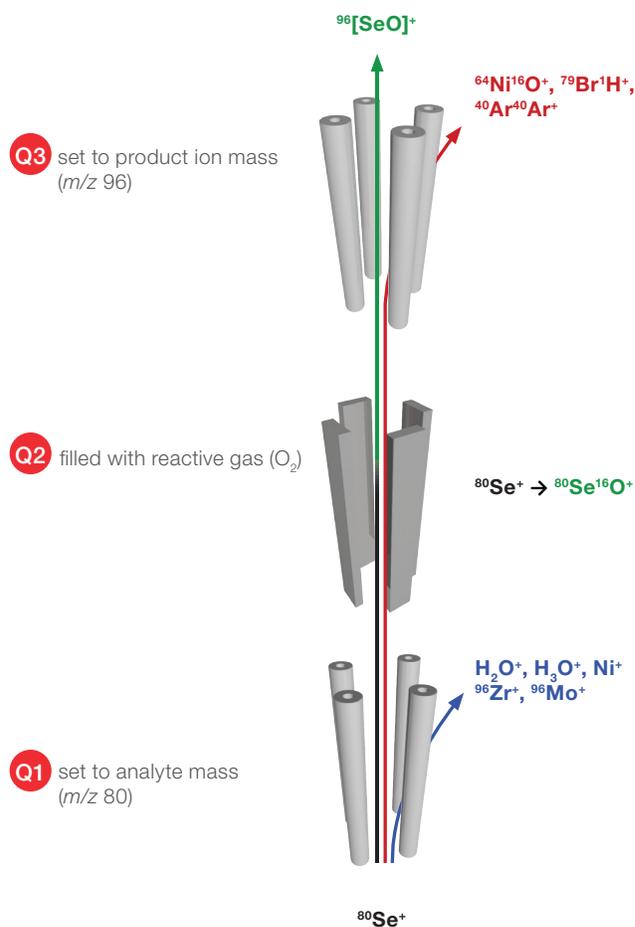
Figure 1. Interference removal for ^{80}Se in the presence of large amounts of nickel using TQ-O$_2$ mass shift mode.

Instrumentation and sample preparation

All measurements were performed using an iCAP TQ ICP-MS, operated using the Qtegra ISDS Software. All samples were prepared using single element standards that were diluted to the concentrations mentioned in the text. Calibration for all analytes (arsenic, cadmium and selenium) were generated in the concentration range between 100 and 1,000 ng·L^{-1} in the corresponding sample matrix (e.g. 100 mg·L^{-1} nickel). Since the calibration was matrix matched, no internal standard was added.

Results

Selenium in nickel alloys

Selenium is an element generally considered as difficult to analyze using ICP-MS for a variety of reasons. First, due to its elevated first ionization potential of 9.75 eV, the ion yield is relatively low and hence the general detection sensitivity is lower compared to elements with low ionization potentials. Second, the main isotopes of selenium are heavily interfered with by argon based polyatomic interferences such as $^{40}Ar_2^+$ on $^{80}Se^+$ or $^{40}Ar^{38}Ar^+$ on $^{78}Se^+$. Commonly, such interferences can be reduced or eliminated using an inert collision gas such as helium and kinetic energy discrimination (KED). However, in the case of a nickel matrix, additional polyatomic interferences occur on the different Se isotopes, with the (lower abundance) ^{82}Se isotope being the least interfered. If bromine is also present (a likely occurrence if high purity hydrochloric acid is used in the sample preparation),

yet another interference is generated ($^{81}Br^1H^+$), which limits the effective use of $^{82}Se^+$. A complete overview of the interferences described above is given in Table 1.

Using SQ operation with a reactive gas such as O_2 or H_2 in the CRC, should theoretically overcome this problem as Se^+ is converted into SeO^+, whereas NiO^+ does not undergo the same reaction. With H_2, NiO^+ ions are neutralized by a charge transfer reaction and therefore eliminated from the ion beam.

However, as can be seen in Figures 2 and 3, both these SQ approaches do not improve the overall detection of selenium in a nickel matrix. The NiO derived interferences cannot be completely removed due to the high amount of Ni present in the sample matrix.

Table 1. Available Isotopes, corresponding abundances and interferences for selenium

Isotope	Abundance	Normal Matrix	Ni Matrix	Bromine
74	0.9		$^{58}Ni^{16}O$	
76	9.00	$^{40}Ar^{36}Ar$	$^{60}Ni^{16}O$	
77	7.60	$^{40}Ar^{37}Cl$	$^{60}Ni^{16}O^1H$	
78	23.60	$^{40}Ar^{38}Ar$, ^{78}Kr	$^{62}Ni^{16}O$	
80	49.70	$^{40}Ar^{40}Ar$, ^{80}Kr	$^{64}Ni^{16}O$	$^{79}Br^1H$
82	9.20	^{82}Kr	$^{64}Ni^{18}O$, $^{64}Ni^{17}O^1H$	$^{81}Br^1H$

Parameter	Value	Confidence Delta at 90%	StdErr	Rel. StdErr [%]
b	144.339	+/-174.393	106.486	73.775
a	3,250,861.921	+/-0.000	0.000	0.000
R^2	0.367			
BEC	22,522.419 ng/l			
IDL(LOD)	666.626 ng/l			
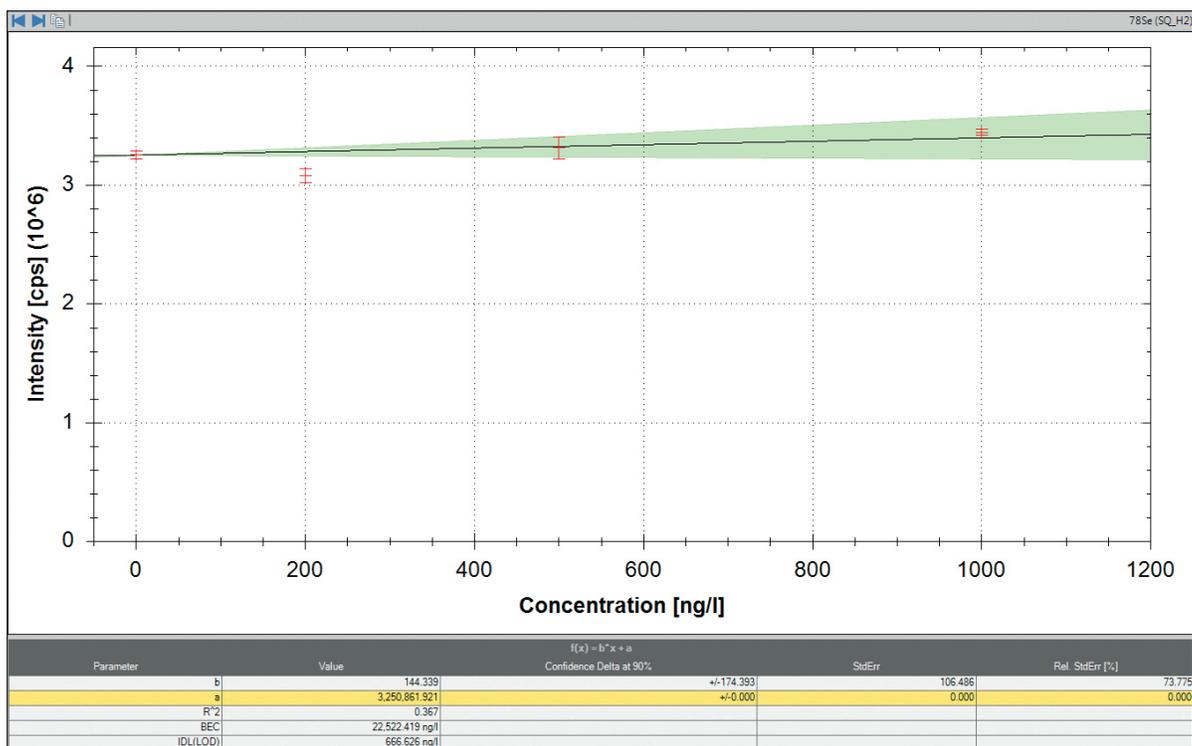
Figure 2. ^{78}Se measured on mass in a 100 mg·L^{-1} nickel solution using SQ mode, with hydrogen cell gas

| Parameter	Value	f(x) = b*x + a Confidence Delta at 90%	StdErr	Rel. StdErr [%]
b	-4.158	+/-4.486	2.739	65.885
a	365,710.443	+/-0.000	0.000	0.000
R^2	0.326			
BEC	-87,955.992 ng/l			
IDL(LOD)	N/A			
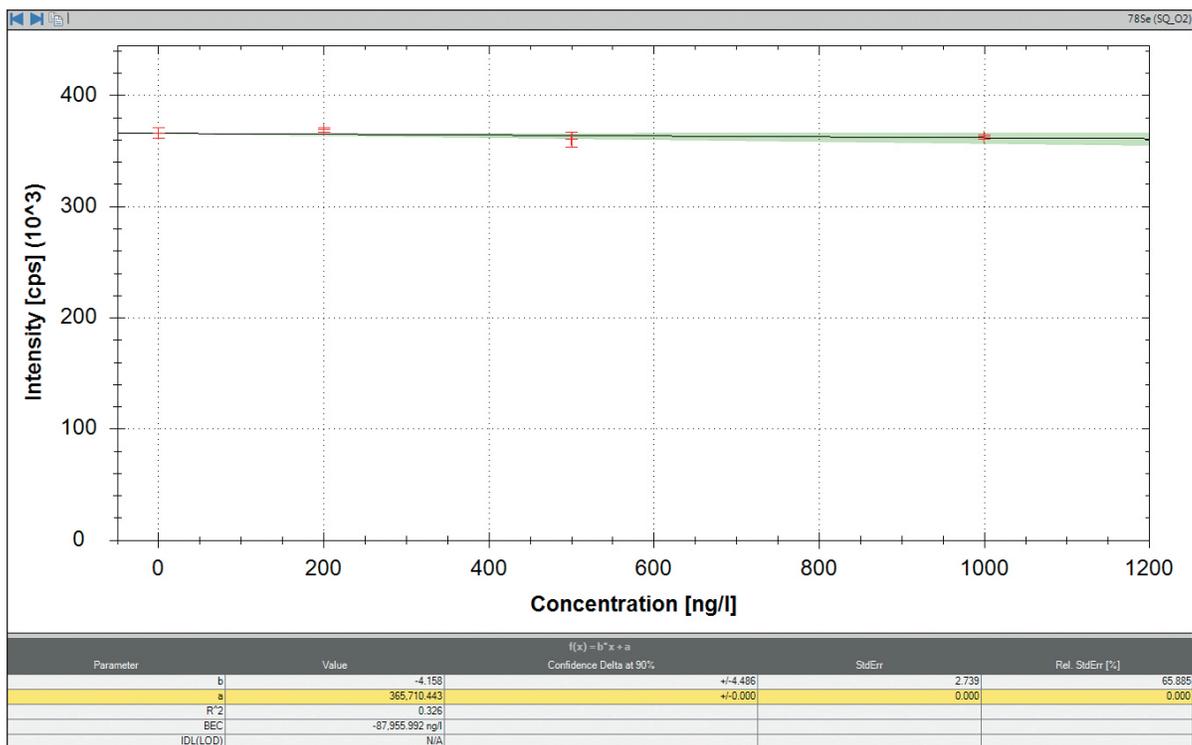
Figure 3. ^{78}Se measured with mass shift mode in a 100 mg·L^{-1} nickel solution using SQ mode, with oxygen cell gas

The reason for this is that apart from the ionic species considered so far, there are other species formed in the plasma which can undergo reactions in the cell. Using the Q1 as an ion guide only, and hence not excluding any ions from the original ion beam, leads to the formation of other unwanted ion clusters, which subsequently hamper the detection of the target analyte. Apart from the most abundant argon based cluster ions (ArAr$^+$, ArO$^+$, ArCl$^+$ etc.), water ions such as H$_2$O$^+$ or H$_3$O$^+$ are formed at very high levels in the plasma and during the transition of the ion beam through the interface region. These water based ions can then be neutralized by various collisions in the cell and then cluster with NiO$^+$ ions to generate new interferences such as NiO(H$_2$O)$^+$ and NiO(H$_3$O)$^+$, which interfere with the mass range between 92-99, thereby coinciding with SeO$^+$ product ions. A summary of all these new interferences is given in Table 2. Since the use of reactive gases to generate product ions (such as O$_2$ to generate SeO$^+$) typically requires ion extraction from the CRC using a non-KED approach (i.e. no voltage barrier between the CRC and the analyzer quadrupole), unintentionally formed ions are also transmitted at a high level. The use of reactive gas settings and SQ operation is therefore ineffective and does not solve the analytical problem. Ions derived from ^{74}Se$^+$ have little analytical value due to their low abundance and as such are not considered.

Table 2. Interferences based on Ni oxides and water cluster ions

Ion Mass	Identifier	Interference
92	^{76}Se^{16}O$^+$	^{58}Ni^{16}O(H$_2$O)$^+$
93	^{77}Se^{16}O$^+$	^{58}Ni^{16}O(H$_3$O)$^+$
94	^{78}Se^{16}O$^+$	^{60}Ni^{16}O(H$_2$O)$^+$, ^{58}Ni^{18}O(H$_2$O)$^+$
96	^{80}Se^{16}O$^+$	^{62}Ni^{16}O(H$_2$O)$^+$, ^{60}Ni^{18}O(H$_2$O)$^+$
98	^{82}Se^{16}O$^+$	^{64}Ni^{16}O(H$_2$O)$^+$, ^{62}Ni^{18}O(H$_2$O)$^+$

With TQ operation, H$_2$O$^+$ and H$_3$O$^+$ are rejected (together with nickel) using Q1, so are not available to react with NiO$^+$. In addition, also nickel precursor ions are eliminated, so that the formation of NiO$^+$ through the use of O$_2$ as a reaction gas is equally eliminated. This is highlighted in Figure 1, showing how the technique can fully remove nickel based polyatomic interferences from the ^{80}Se isotope.

In the first quadrupole (Q1), Se is filtered from other interfering elements or molecules such as H$_2$O$^+$ or H$_3$O$^+$ and also ^{96}Zr$^+$ and ^{96}Mo$^+$. In the CRC (Q2), Se$^+$ can react with O$_2$ to form SeO$^+$, whereas the main interference, ^{60}Ni^{18}O$^+$, does not further react and can therefore be eliminated in a second mass filtering quadrupole (Q3).

Parameter	Value	Confidence Delta at 90%	StdErr	Rel. StdErr [%]
b	4.508	+/-0.033	0.020	0.442
a	209.802	+/-0.000	0.000	0.000
R^2	1.000			
BEC	46.537 ng/l			
IDL(LOD)	12.884 ng/l			
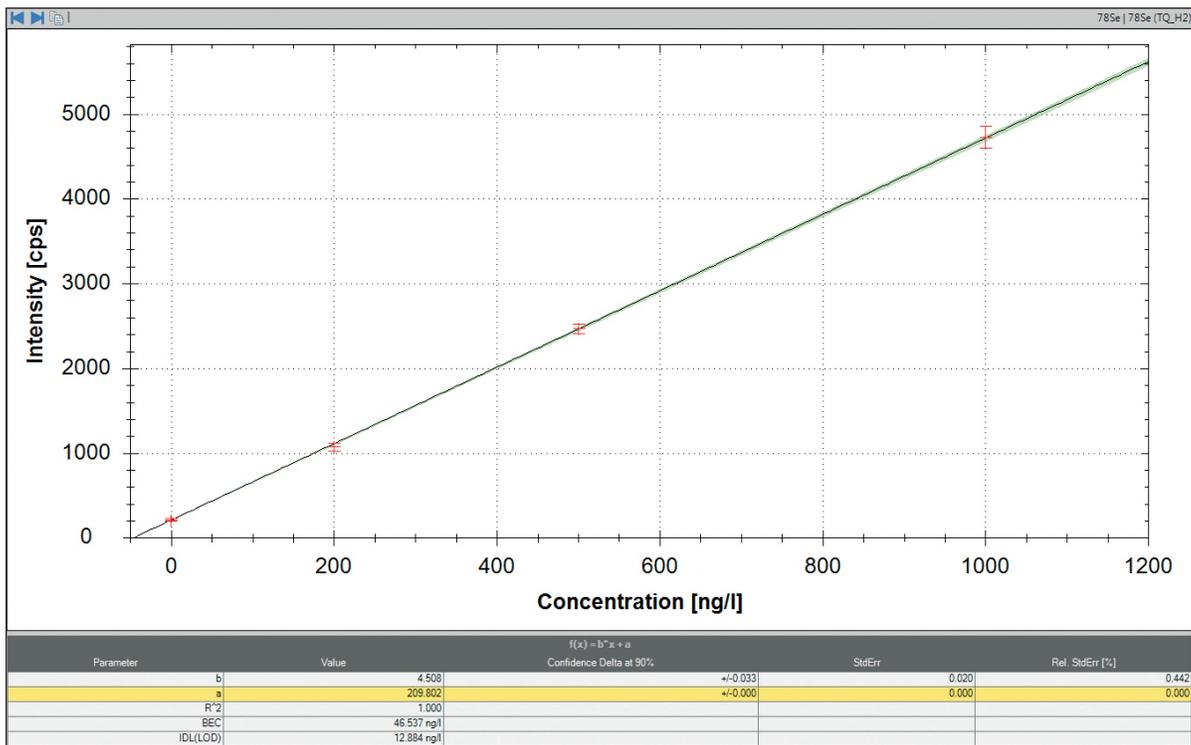
Figure 4. ^{78}Se measured in a 100 mg·L^{-1} nickel solution using TQ-H$_2$ on mass mode

Parameter	Value	Confidence Delta at 90%	StdErr	Rel. StdErr [%]
b	1.003	+/-0.008	0.005	0.457
a	47.900	+/-0.000	0.000	0.000
R^2	1.000			
BEC	47.775 ng/l			
IDL(LOD)	18.790 ng/l			
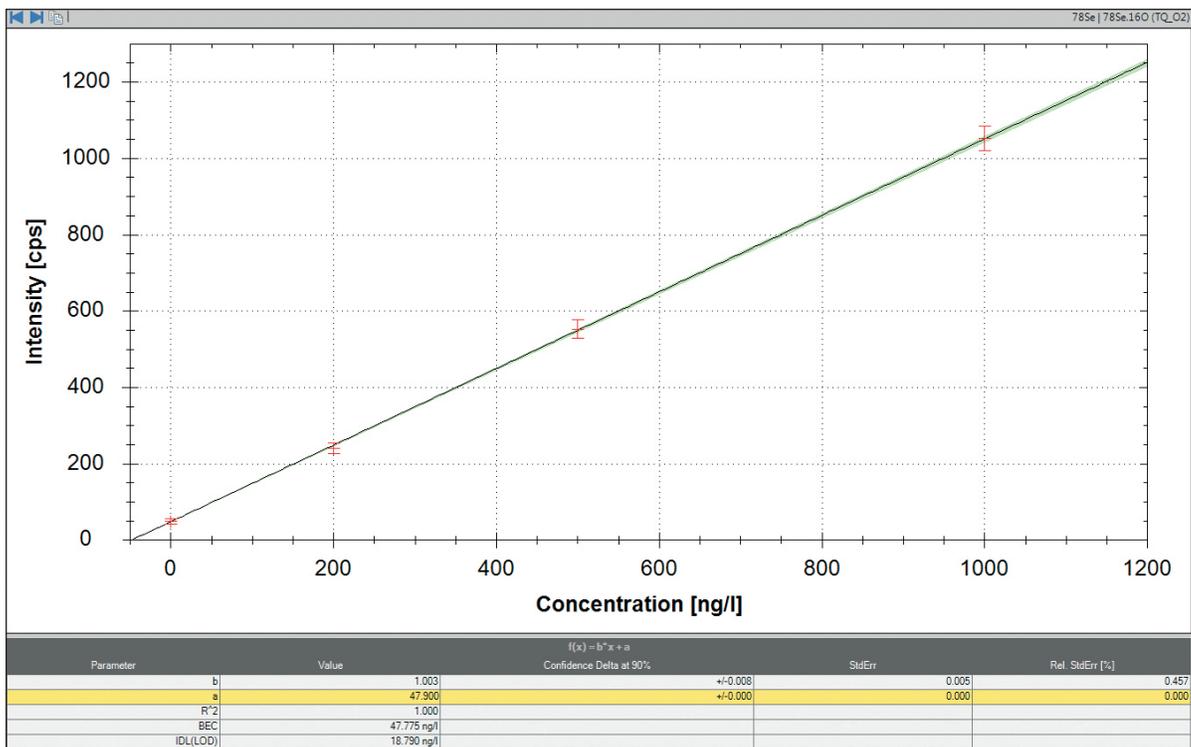
Figure 5. ^{78}Se measured in a 100 mg·L^{-1} nickel solution using TQ-O$_2$ mass shift mode

Parameter	Value	f(x) = b*x + a Confidence Delta at 90%		StdErr	Rel. StdErr [%]
b	9.701	+/-0.097		0.059	0.608
a	376.906	+/-0.000		0.000	0.000
R^2	1.000				
BEC	38.854 ng/l				
IDL(LOD)	10.548 ng/l				
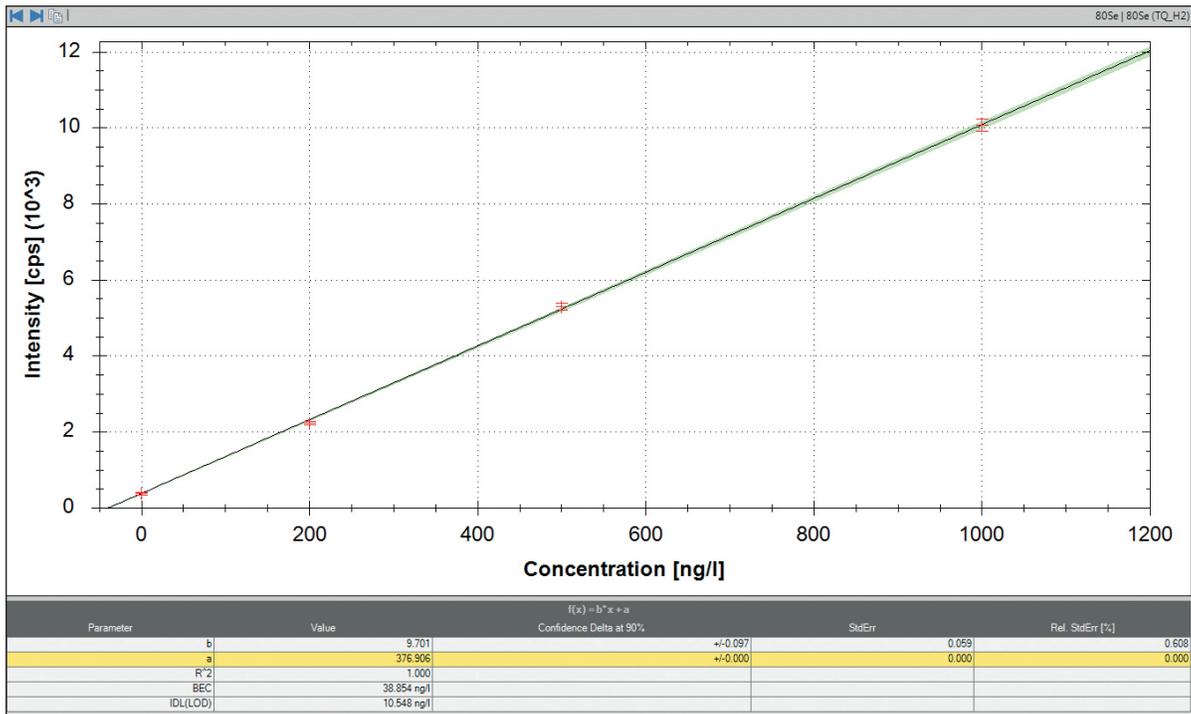
Figure 6. ^{80}Se measured in a 100 mg·L^{-1} nickel solution using TQ-H$_2$ on mass mode

| Parameter	Value	f(x) = b*x + a Confidence Delta at 90%		StdErr	Rel. StdErr [%]
b	2.200	+/-0.027		0.017	0.751
a	29.000	+/-0.000		0.000	0.000
R^2	1.000				
BEC	13.184 ng/l				
IDL(LOD)	5.103 ng/l				
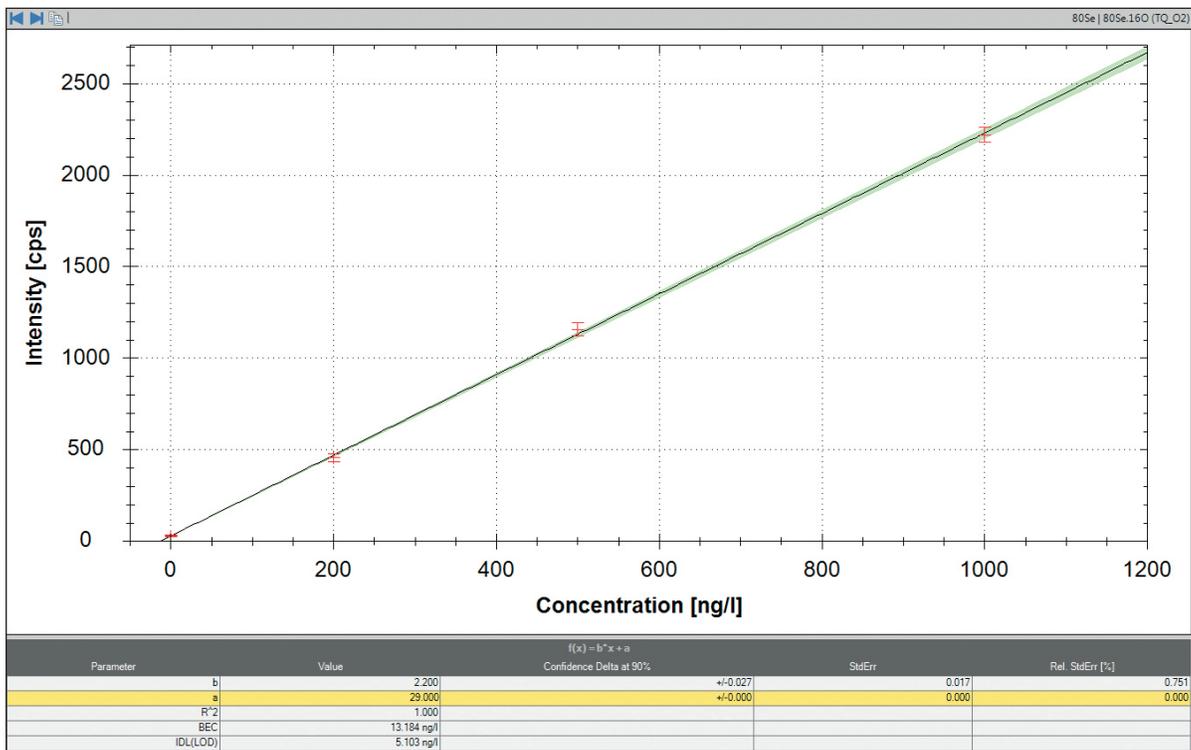
Figure 7. ^{80}Se measured in a 100 mg·L^{-1} nickel solution using TQ-O$_2$ mass shift mode

The resulting calibration curves for selenium in a nickel matrix (Figures 4, 5, 6 and 7) show that all interferences have been fully eliminated independent of whether O_2 or H_2 have been used as reactive gases. This again highlights that the main reason why SQ modes fail for this analysis is not because of inefficient removal of the original interference (NiO), but rather the creation of additional interferences inside the CRC as a result of gas phase ion-molecule reactions with other species derived from the sample.

The analytical figures of merit for the different modes are summarized in Table 3. As can be seen, the use of H_2 as a reactive gas leads to a higher attainable detection sensitivity, but is not as efficient as O_2 for the removal of all NiO based interferences. The efficiency is shown by the background equivalent concentration (BEC) for H_2 gas being slightly elevated in comparison to the O_2 results. For both modes, the limit of detection is in a similar range, being between 5 and 10 ng·L^{-1} for $^{80}Se^+$.

Table 3. Analytical figures of merit for the analysis of Se in a 100 mg·L^{-1} nickel matrix

MODE/isotope	Sensitivity (cps·L·μg^{-1})	BEC (ng·L^{-1})	IDL (ng·L^{-1})
TQ-H$_2$			
$^{78}Se^+$	4,500	46.5	12.9
$^{80}Se^+$	9,700	38.9	10.5
TQ-O$_2$			
$^{78}Se^+$	1,000	47.8	18.8
$^{80}Se^+$	2,200	13.2	5.10

Arsenic and cadmium in zirconium alloys

With samples containing elevated levels of zirconium, the analysis of $^{111}Cd^+$ and $^{113}Cd^+$ is compromised through the formation of ions such as $^{94}Zr^{16}O^1H^+$. Additionally, impurities of tin and indium result in isobaric interferences on all the remaining cadmium isotopes.

When analyzed using SQ-ICP-MS, arsenic is generally measured using pure helium as a collision cell gas with KED, an approach that ensures consistent removal of polyatomic interferences such as $^{40}Ar^{35}Cl^+$, which would interfere with the only isotope for arsenic at m/z 75.

When analyzed using O_2 in the CRC, $^{75}As^+$ is converted into $^{75}As^{16}O^+$, which is subsequently detected at m/z 91 as the product ion mass. This mass however is strongly interfered by $^{90}Zr^1H^+$. Using SQ-ICP-MS with O_2 as a reaction gas would promote the formation of ZrO, leading to a mass shift of the interference as well as the analyte.

The corresponding calibration curves for arsenic in a matrix of 100 ppm of zirconium in SQ-KED and TQ-O_2 mode are shown in Figures 8 and 9. For this particular analyte/matrix combination, there is no apparent difference between both modes; however, the attainable detection sensitivity is higher for TQ-O_2, whereas similar ranges for BEC's (approximately 80 ng·L^{-1}) and LOD's (between 8 and 17 ng·L^{-1}) are observed (Table 4).

| | | f(x) = b*x + a | | | |
Parameter	Value	Confidence Delta at 90%	StdErr	Rel. StdErr [%]
b	5.905	+/-0.008	0.005	0.086
a	473.159	+/-0.000	0.000	0.000
R^2	0.99999			
BEC	80.1 ng/l			
IDL(LOD)	16.7 ng/l			
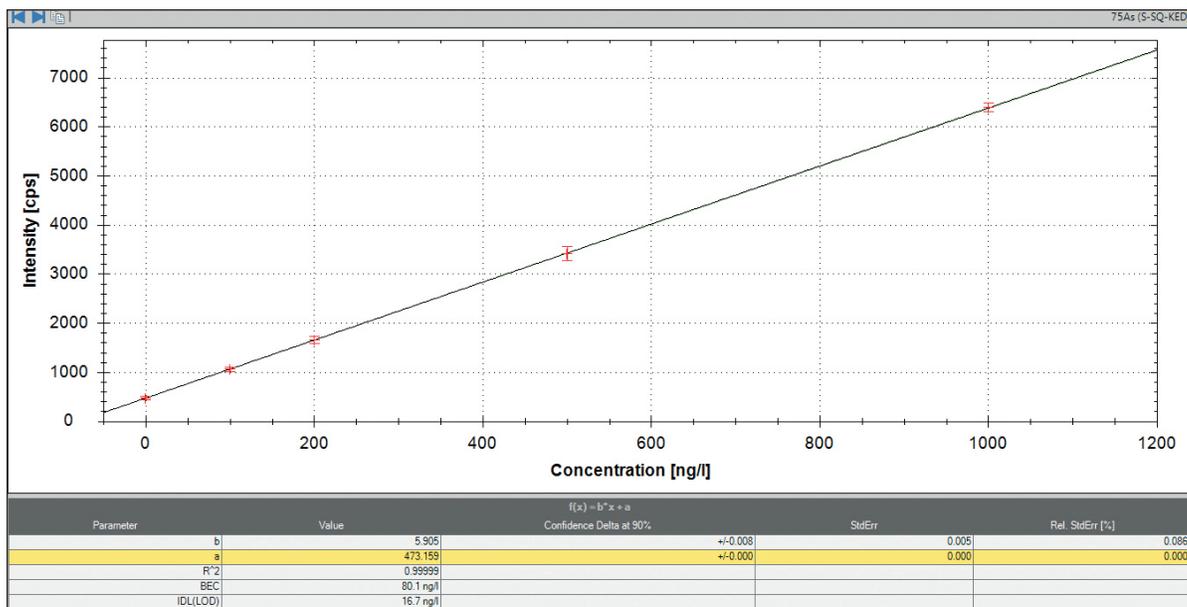
Figure 8. Calibration curve for arsenic in a 100 mg·L^{-1} zirconium matrix using helium as a cell gas and SQ-KED
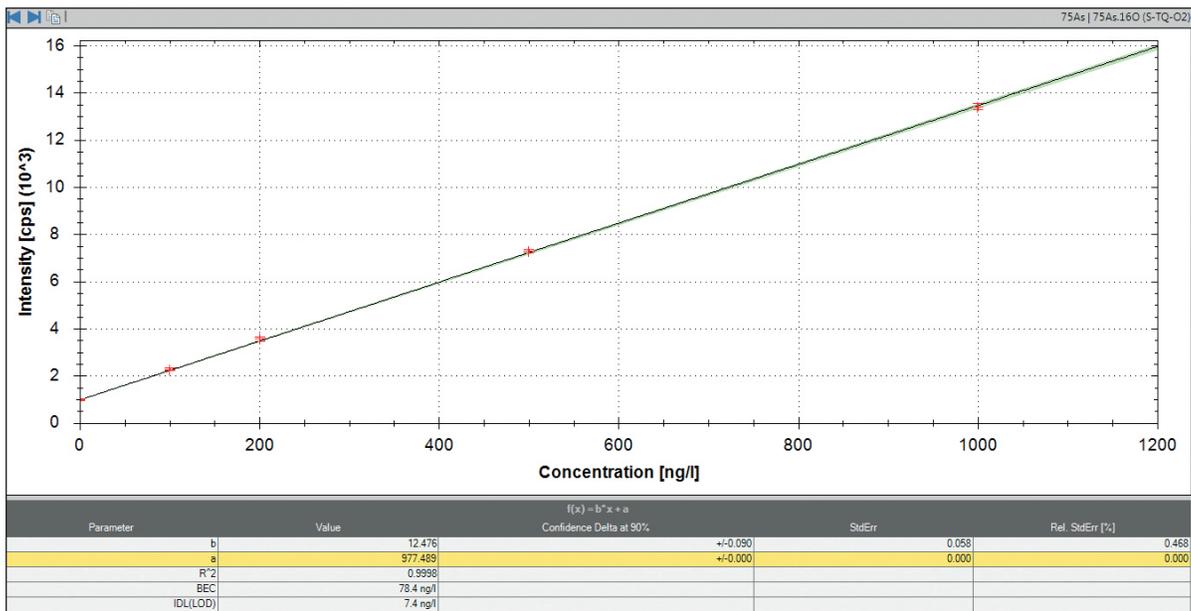
Figure 9. Calibration curve for arsenic in a 100 mg·L^{-1} zirconium matrix using TQ-O$_2$ mass shift mode

Table 4. Analytical figures of merit for the analysis of arsenic and cadmium in a 100 mg·L^{-1} zirconium 1 mg·L^{-1} Sn matrix

MODE/isotope	Sensitivity (cps·L·µg^{-1})	BEC (ng·L^{-1})	IDL (ng·L^{-1})
SQ-KED			
^{75}As$^+$	5,900	80.1	16.7
^{111}Cd$^+$	3,600	5,000	1,000
TQ-O$_2$			
^{75}As$^+$	12,500	78.4	7.4
^{111}Cd$^+$	4,500	10.6	1.7

Table 5. Available Isotopes, corresponding abundances and interferences for cadmium

Isotope	Abundance	Interference
^{106}Cd$^+$	1.25	^{90}Zr^{16}O$^+$
^{108}Cd$^+$	0.89	^{92}Zr^{16}O$^+$, ^{90}Zr^{18}O$^+$
^{110}Cd$^+$	12.49	^{94}Zr^{16}O$^+$, ^{92}Zr^{18}O$^+$
^{111}Cd$^+$	12.80	^{94}Zr^{16}O^{1}H$^+$
^{112}Cd$^+$	24.13	^{96}Zr^{16}O$^+$, ^{94}Zr^{18}O$^+$, ^{112}Sn$^+$
^{113}Cd$^+$	12.22	^{96}Zr^{16}O^{1}H$^+$, ^{113}In$^+$
^{114}Cd$^+$	28.73	^{96}Zr^{18}O$^+$, ^{114}Sn$^+$
^{116}Cd$^+$	7.49	^{116}Sn$^+$

Cadmium has a large number of isotopes (Table 5), where ^{111}Cd is the best candidate for direct analysis, as it is not directly interfered either through a ZrO derived interference (the level of hydroxide derived interferences is generally lower) nor through a tin or indium derived isobaric interference. All other isotopes are either directly interfered through a polyatomic ZrO interference, or show an isobaric interference with tin or indium.

As mentioned previously, the use of SQ-KED is a tool that efficiently removes polyatomic species such as oxide interferences when these interferences are not excessively high. With high concentrations of zirconium in the sample matrix, the contribution of ^{94}Zr^{16}O^{1}H$^+$ cannot be fully eliminated using SQ-KED, as demonstrated by the calibration curve in Figure 10. Figure 11 shows a full mass scan over the region between masses 86 and 130 illustrating the overall interference profile on cadmium. The isotopic pattern of the signals observed in the mass range between 106 and 112 clearly reflects the isotopic pattern of zirconium and therefore confirms the presence of ZrO species at these masses.

Parameter	Value	f(x) = b*x + a Confidence Delta at 90%	StdErr	Rel. StdErr [%]
b	36.502	+/-3.381	2.205	6.040
a	185,534.867	+/-0.000	0.000	0.000
R^2	0.9672			
BEC	5,082.8 ng/l			
IDL(LOD)	1,082.6 ng/l			
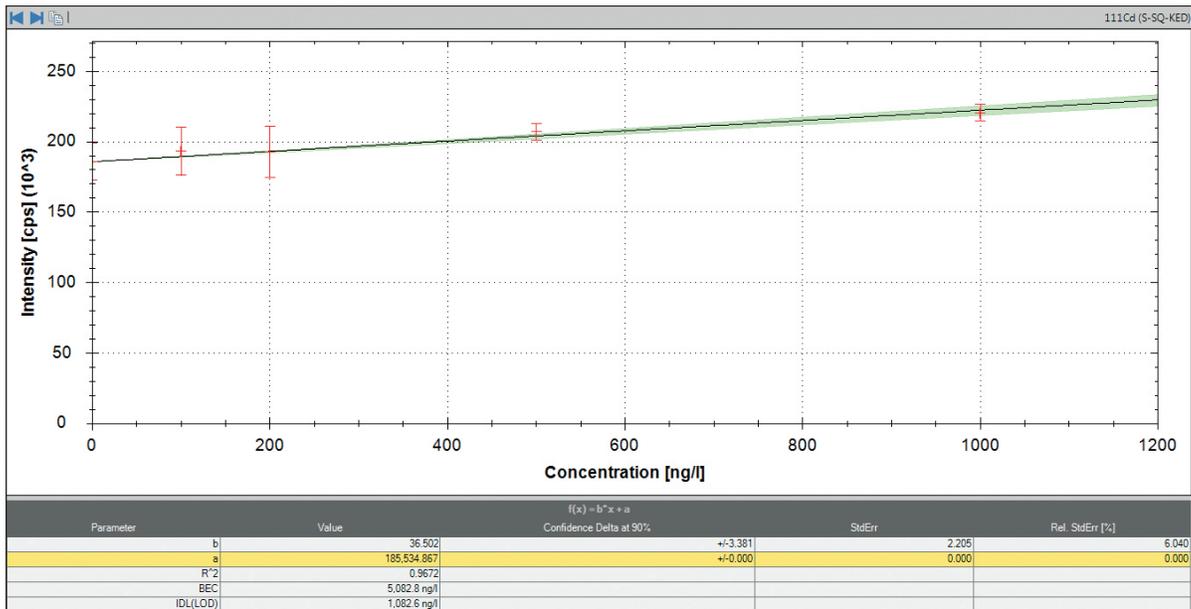
Figure 10. Calibration curve for ^{111}Cd in a 1,000 mg·L^{-1} zirconium sample matrix using SQ-KED
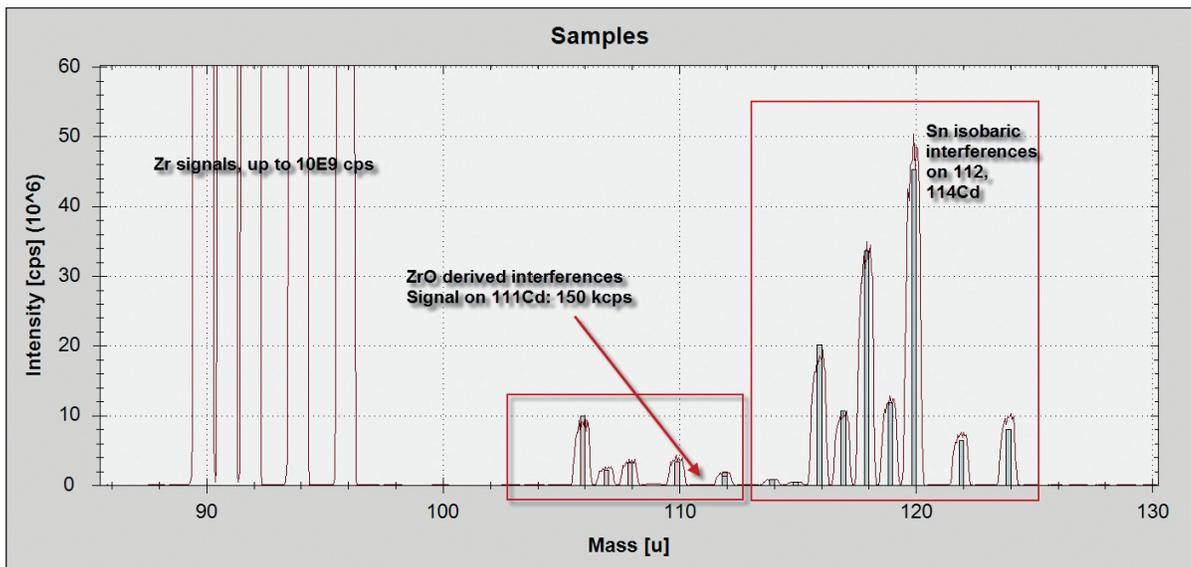
Figure 11. Full mass spectrum showing signals caused by the sample matrix 100 mg·L^{-1} of zirconium with 1 mg·L^{-1} of tin. No cadmium was added to this solution.

One approach to eliminate zirconium related interferences on cadmium is to use O_2 in the CRC and to fully oxidize incoming ZrO ions to ZrO_2. At the same time, cadmium does not react and can therefore be measured interference free on its original ion mass. This is commonly referred to as TQ on mass mode (Figure 12).

Figure 12. Interference removal for ^{111}Cd in the presence of large amounts of zirconium and tin using TQ-O$_2$ on mass mode
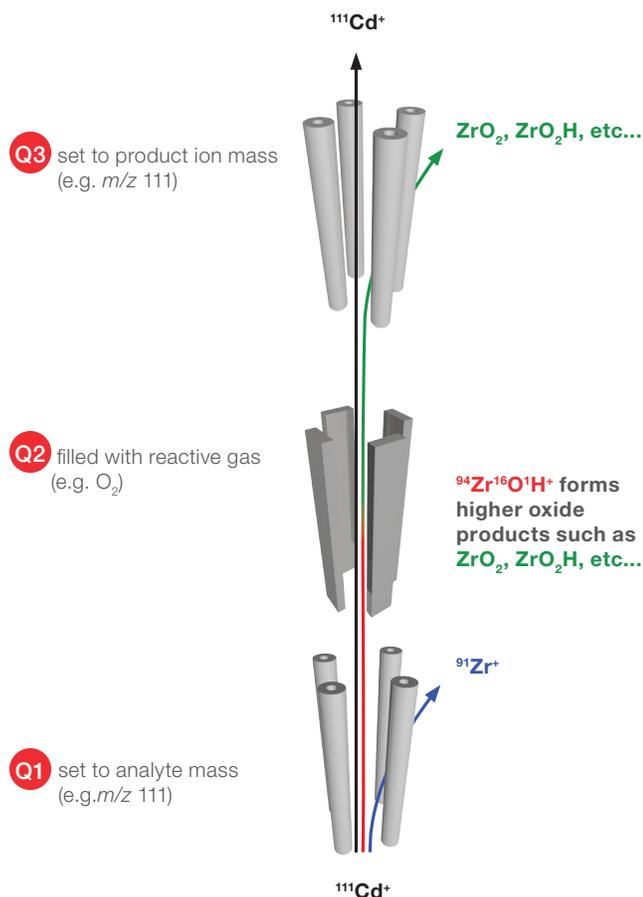
The general working principle of a TQ-ICP-MS system in TQ on mass mode is:

Q1 is set to transmit the original mass of the target analyte. In this case, interfering ions at the same mass will also enter the CRC.

Q2 promotes the reaction of interfering ions with the reaction gas to form product ions with higher mass to charge ratios than the original interfering ion. The analyte does not react under these conditions.

Q3 is set to the same mass as Q1, so that only the analyte is allowed to reach the detection system.

Using the TQ-O$_2$ mode, all interfering ZrO derived species on the target isotope of Cd are eliminated, leading to an interference free detection. Since only one interfering ion for $^{111}Cd^+$ ($^{94}Zr^{16}O^1H^+$) is allowed to enter the CRC, it can be fully oxidized and is therefore eliminated, while unreactive $^{111}Cd^+$ is detected via its original isotope mass of 111. This is reflected in the low BEC value achieved using the TQ-O$_2$ mode of about 11 ng·L^{-1} and the attainable LOD of 1.7 ng·L^{-1} (Table 4).


Figure 13. Calibration curve for ^{111}Cd in a 1,000 mg·L^{-1} Zr sample matrix using TQ-O$_2$ on mass mode

Conclusion

The iCAP TQ ICP-MS is capable of resolving interferences created by very complex matrices. As shown, it is not always sufficient to remove the most obvious interferences for a given analyte, as the ICP ion source may also contain other species which contribute to interferences. These species may not directly create an interference with the analyte in the plasma, but may undergo reactions in the CRC that generate additional interferences that then severely compromise the achievable detection limit. The use of reactive gases in combination with a mass filtering step in Q1 to remove other unwanted ions is therefore the ideal solution for this analytical problem.

At the same time, the use of TQ-ICP-MS offers two effective ways for interference removal, namely TQ mass shift and TQ on mass modes, to enable accurate analysis. With the iCAP TQ ICP-MS, selection of the most appropriate mode of analysis and the correct settings for all quadrupoles, gas flows and scan settings is accomplished by the Qtegra ISDS Software and its unique Reaction Finder method development assistant, thereby greatly simplifying the use of powerful triple quadrupole technology for routine applications.

Find out more at **thermofisher.com/TQ-ICP-MS**

ThermoFisher
SCIENTIFIC